

# Uplink Channel Estimation and Signal Extraction Against Malicious Intelligent Reflecting Surface in Massive MIMO System

Xiaofeng Zheng, Ruohan Cao

**Abstract**—This paper investigates the effect of malicious intelligent reflecting surfaces (IRSs) in a massive MIMO uplink. The IRSs are used by malicious users (MUs) for randomly reflecting pilot and data sequences of legitimate users (LUs) to a base station (BS), we consider the problem of channel estimation and signal extraction in the presence of the malicious IRSs. Firstly, we find that by using the IRSs, the reflected sequences are correlative to the data sequences of LUs. This correlation challenges traditional channel estimation techniques. To be more precisely, we prove that the right singular matrix of a received signal at the BS is a function of the correlation between the legitimate and reflection data in a large-scale antenna regime. As a result, the correlation caused by malicious IRSs degrades the performance of traditional channel estimation methods based on eigenvalue decomposition (EVD) of the received signals. To address this challenge, we propose a signal extraction and channel estimation method to combat malicious IRSs. More precisely, geometric arguments, such as convex hulls of extracted signals exhibit insensitive to the correlation. The convex hulls are thus utilized to provide signal extraction and channel estimation criteria. To optimize these criteria, we develop an extractor that can capture the convex hulls of desired signals from noisy signals. Based on this, we formulate two optimization problems, whose global minima are solved to perform signal extraction and channel estimation. Experimental results show that when the IRSs randomly flop reflection phases with probability of 0.8, the proposed method outperforms the EVD-based method by more than 5 dB in the sense of normalized mean square error (NMSE).

**Index Terms**—Malicious attack, uplink channel estimation, massive MIMO, intelligent reflecting surface

## I. INTRODUCTION

Massive multiple-input and multiple-output (MIMO) is a key technology in fifth-generation (5G) communication that can achieve high speed and large capacity [1]. Its advantage depends on trustworthy channel state information (CSI) [2]. Nevertheless, malicious users (MUs) may exist in 5G networks, and they may actively send interference to disturb channel estimation. As a result, trustworthy CSI cannot be obtained, and false CSI undermines the performance of a massive MIMO system. To obtain trustworthy CSI, it is important to investigate channel estimation under malicious attack [3].

Much work has investigated channel estimation under malicious attack. This work differs in the underlying assumptions

of the attack model. For instance, in some work, MUs do not know the pilot sequences (PSs) employed by legitimate users (LUs), and must send random PSs to disturb channel estimation [4]–[6]. In one case [4], a single LU and a base station (BS) share a secret PS that is unknown to another MU. The null space of the secret PS is used to eliminate the LU's pilot signal received at the BS, while leaving the pilot signal of the MU. As a beneficial result, the channel of the MU is estimated based on the remaining pilot signal. In another study [5], all LUs and MUs select random PSs from a well-known pilot codebook that consists of orthogonal PSs. The BS does not know the selected PSs. It projects its received pilot signal onto the pilot codebook and estimates the selected PSs from its projection. With the estimation of the selected PSs, channel estimation is achieved. In another study [6], LUs and MUs independently send random symbols. The independence applies independent component analysis (ICA) to channel separation, which finally leads to channel estimation. Similarly, two-stage uplink training was proposed [7], assuming that the powers of LUs are different during the two stages, while they are invariable in two stages. This assumption of different power facilitates channel estimation.

The above methods are implemented during the pilot phase, requiring some additional pilot signal protocols which are unknown to the MUs. Other work estimates channels during the data phase [8] [9]. More precisely, they employ eigenvalue decomposition (EVD) to signals received through the data phase. Based on the resulting eigenspace, channels of LUs and MUs can be separated in probability as the number of antennas approaches infinity [8] [9]. With these separated channels, the transmission power gap between LUs and MUs is further used for channel identification. We note that a key assumption enabling the EVD-based method is that the jamming and data sequences are statistically independent. Without this assumption, the performance of EVD-based methods cannot be guaranteed.

In summary, current work requires either additional pilot protocols [4]–[7] or independence between sequences of LUs and MUs [8] [9]. However, due to size or resource constraints of mobile users in the internet of things (IoT), additional pilot protocols may not always be available. On the other hand, as an emerging device, the IRSs have a wide range of application in IoT [10]. When IRS is utilized for attack by MUs, the independence between sequences of MUs and LUs may change, which may undermine the performance of EVD-based methods [8] [9]. Although there many works on security

X. Zheng and R. Cao are with the Key Laboratory of Trustworthy Distributed Computing and Service, Ministry of Education, and also the School of Information and Communication Engineering, Beijing University of Posts and Telecommunications (BUPT), Beijing 100876, China (e-mail: {zhengxiaofeng, caoruohan}@bupt.edu.cn).

techniques with IRS [11] [12], to the authors' best knowledge, it is sparse to consider the effect of IRS used for attack, and countermeasures to such attack as well.

Against this background, we consider combat against attack conducted by IRSs. We propose a channel estimation and signal extraction method that requires no additional pilot protocol. The main contributions of the paper are as follows.

- 1) We first find that the malicious IRSs could cause correlative attack in the sense that the reflected sequences are *correlative* to the data sequences of LUs. Then, Proposition 1 characterizes the effect of correlative attack. We obtain that the right singular matrix of the received signal at the BS is a function of the correlation between legitimate and jamming data sequences in a large-scale antenna regime. More precisely, when EVD is applied to the received signals, the eigenspaces corresponding to the MUs and LUs overlap. As a result, the interference cannot be eliminated by the eigenspace, which degrades the performance of traditional EVD-based methods in the presence of *correlative* attacks.
- 2) To combat *correlative* attacks caused by the malicious IRSs, we use a geometric argument to develop signal extraction and channel estimation criteria. Our geometric argument is robust to a correlative attack, but sensitive to noise. To optimize the proposed criteria, Proposition 2 presents an extractor that can identify geometric properties of desired signals from noisy observations, by which we achieve signal extraction and channel estimation in the presence of *correlative* attacks by solving two optimization problems.

The rest of this paper is organized as follows. Section II presents the attack model about the MU equipped with IRS. Section III analyses the attack strategies and effects caused by IRS. In Section IV, we propose the signal extraction and channel estimation method in the presence of *correlative* attacks. Simulation results are provided in Section V, and conclusions are drawn in Section VI.

*Notation:* Vectors are denoted by lowercase italicized letters, and matrices by uppercase italicized letters. A superscript  $(\cdot)^T$  indicates a matrix transpose. We use  $\text{tr}(\mathbf{A})$  to denote the trace of matrix  $\mathbf{A}$ , and  $[\cdot]_m$  denotes the  $m$ th row of an input matrix or vector.  $P_X$  denotes the stochastic distribution of the random variable  $X$ ,  $P_X(x) = \Pr(X = x)$ .  $P_{AB}$  denotes the joint distribution of random variables  $A$  and  $B$ .  $\odot$  denotes a dot product.  $X \xrightarrow{a.s.} Y$  indicates that  $X$  converges to  $Y$  almost surely, where  $X$  and  $Y$  are generic random variables or bounded constants.  $\|\cdot\|_2$  denotes the 2-norm.

## II. SYSTEM MODEL

In Fig. 1, we consider a system model including a BS equipped with  $M$  antennas,  $N$  single-antenna LUs, and  $N$  MUs, where the  $j$ th LU is attacked by the  $j$ th MU during the pilot and data phases,  $j = 1, 2, \dots, N$ . This assumption also follows refers. [13]. Each MU is equipped with an IRS that includes  $W$  elements. The uplink communication between the BS and the LUs takes place in two phases, the pilot and data phases, including  $L_p$  and  $n$  instants, respectively. During the

two phases, the MUs reflect spoofed PSs and signal sequence with the LUs to the BS. More precisely, during the pilot phase, the IRSs of MUs reflect the PSs without any phase-shift, and during the data phase, the MUs reflect information data sequences with a random phase shift.

In the pilot phase, the  $j$ th LU transmits the PS  $\mathbf{x}_j \in \mathbb{C}^{1 \times L_p}$ , which is selected from a public pilot codebook  $\mathbf{X}$ . We assume the MUs conduct pilot attack, so we define a diagonal matrix  $\Phi_p = \text{diag}(1, \dots, 1)$ ,  $\Phi_p \in \mathbb{C}^{W \times W}$ , as the reflection-coefficient matrix of the IRS about the  $j$ th MU, which means the MUs reflect the same PS with the LUs. The received signals  $\mathbf{Y}_p \in \mathbb{C}^{M \times L_p}$  in the pilot phase can be specified as

$$\begin{aligned} \mathbf{Y}_p &= \sum_{j=1}^N (\mathbf{h}_j \mathbf{x}_j + \mathbf{G}_{j_2} \Phi_p \mathbf{g}_{j_1} \mathbf{x}_j) + \mathbf{N}_p \\ &= \sum_{j=1}^N (\mathbf{h}_j \mathbf{x}_j + \sum_{w=1}^W \mathbf{g}_{j_w} \mathbf{x}_j) + \mathbf{N}_p, \end{aligned} \quad (1)$$

where  $\mathbf{h}_j$  denotes the channel from the  $j$ th LU to the BS,  $\mathbf{h}_j \in \mathbb{C}^{M \times 1}$ ;  $\mathbf{g}_{j_1}, \mathbf{G}_{j_2}$  respectively denote the channels from the  $j$ th LU to the  $j$ th MU and from the  $j$ th MU to the BS,  $\mathbf{g}_{j_1} = [g_{j_1}(1), \dots, g_{j_1}(W)]^T \in \mathbb{C}^{W \times 1}$ ,  $g_{j_1}(w) \in \mathbb{C}^{1 \times 1}$ ,  $g_{j_1}(w)$  denotes the channel from the  $j$ th LU to the  $w$ th element of the  $j$ th MU.  $\mathbf{G}_{j_2} = [\mathbf{g}_{j_2}[1], \dots, \mathbf{g}_{j_2}[W]] \in \mathbb{C}^{M \times W}$ ,  $\mathbf{g}_{j_2}[w] \in \mathbb{C}^{M \times 1}$ ,  $\mathbf{g}_{j_2}[w]$  denotes the channel from the  $w$ th elements of  $j$ th MU to the BS; and  $\mathbf{g}_{j_w} = \mathbf{g}_{j_2}[w] g_{j_1}(w)$ , denotes the cascaded channels of the  $w$ th element of IRS,  $\mathbf{g}_{j_w} \in \mathbb{C}^{M \times 1}$ .  $\mathbf{N}_p \in \mathbb{C}^{M \times L_p}$  are Gaussian noise, and each element follows  $\mathcal{CN}(0, \sigma^2)$ .

In the data phase, the  $j$ th LU transmits  $\mathbf{a}_j \in \mathbb{C}^{1 \times n}$ . Due to the IRS of MU with  $W$  reflection elements, the MU reflects  $W$  stream signal sequences. We further define the diagonal matrix  $\Phi_j(t) = \text{diag}(e^{i\phi_{j_1}(t)}, \dots, e^{i\phi_{j_W}(t)})$ ,  $1 \leq t \leq n$ ,  $\Phi_j(t) \in \mathbb{C}^{W \times W}$  as the reflection-coefficient matrix of the  $j$ th IRS, which is randomly set according to  $\Pr\{\phi_{j_w}(t) = 0\} = p_w$ ,  $\Pr\{\phi_{j_w}(t) = \pi\} = 1 - p_w$ ,  $1 \leq w \leq W$ . The received signals  $\mathbf{y}(t) \in \mathbb{C}^{M \times 1}$  in the data phase can be specified as

$$\begin{aligned} \mathbf{y}(t) &= \sqrt{P} \sum_{j=1}^N (\mathbf{h}_j \mathbf{a}_j(t) + \mathbf{G}_{j_2} \Phi_j(t) \mathbf{g}_{j_1} \mathbf{a}_j(t)) + \mathbf{N} \\ &= \sqrt{P} \sum_{j=1}^N (\mathbf{h}_j \mathbf{a}_j(t) + \sum_{w=1}^W \mathbf{g}_{j_w} \mathbf{b}_{j_w}(t)) + \mathbf{n}, 1 \leq t \leq n \end{aligned} \quad (2)$$

$$\mathbf{b}_{j_w}(t) = \mathbf{a}_j(t) e^{i\phi_{j_w}(t)}, \quad (3)$$

$\mathbf{b}_{j_w} \in \mathbb{C}^{1 \times n}$ , where  $\mathbf{a}_j(t), \mathbf{b}_{j_w}(t)$  respectively denote the  $t$ th elements in  $\mathbf{a}_j, \mathbf{b}_{j_w}$ .  $\mathbf{n} \in \mathbb{C}^{M \times 1}$  is Gaussian noise, and each element follows  $\mathcal{CN}(0, \sigma^2)$ .  $P$  is the transmission power of each user.

*Remark 1:* Although we consider each LU to be attacked by single MU with  $W$  elements, the model characterized by (2) and (3) is equivalent the two-MU with each having  $\frac{W}{2}$  reflection elements. As such, our proposed technique is extensible for multi-MU model.

### III. ATTACK STRATEGIES AND EFFECTS

#### A. Attack strategies

For the deterministic reflection,  $p_w = 1$  or  $p_w = 0$ , based on (3), the IRSs reflect the same signal or opposite signal with LU. In this case, estimated signal is the mixed of  $\mathbf{a}_j$ .

For the random reflection,  $0 < p_w < 1$  based on (3), we find that  $\mathbf{b}_{j_w}$  and  $\mathbf{a}_j$  are correlation. To be more precisely, we assume that  $\mathbf{a}_j$  is an independent and identically distributed (i.i.d.) sequence. According to (3),  $\mathbf{b}_{j_w}$  is also an i.i.d. sequence. There are random variables  $A$  and  $B$  having the same stochastic distributions as each element of  $\mathbf{a}_j$  and  $\mathbf{b}_{j_w}$ , respectively. Let us use  $P_A$  and  $P_B$  to denote stochastic distributions of  $A$  and  $B$ , respectively.  $\mathcal{A}_j$  and  $\mathcal{B}_{j_w}$  are the alphabets of these two variables,  $a$  and  $b$  denote generic symbols of  $\mathcal{A}_j$  and  $\mathcal{B}_{j_w}$ , respectively. When BPSK modulation is used by the LUs, it is not hard to obtain that  $P_A(1) = P_A(-1) = \frac{1}{2}$ ,  $P_{B|A}(1|1) = P_{B|A}(-1|-1) = p_w$ ,  $P_{B|A}(-1|1) = P_{B|A}(1|-1) = 1 - p_w$ . Therefore,

$$P_{A,B}(1,1) = \frac{1}{2}p_w, P_A(1)P_B(1) = \frac{1}{4}. \quad (4)$$

By designing  $p_w \neq \frac{1}{2}$  in (3), there exists

$$P_{A,B}(a,b) \neq P_A(a)P_B(b), a \in \mathcal{A}_j, b \in \mathcal{B}_{j_w}. \quad (5)$$

(5) shows that  $\mathbf{a}_j(t), \mathbf{b}_{j_w}(t)$  are *correlative*, and we refer the attack caused by IRS as a *correlative* attack. Reflection coefficient affects the correlation between signals,

As indicated by (4), when  $p_w \neq \frac{1}{2}$ ,  $P_{A,B}(1,1) \neq P_A(1)P_B(1)$ . We further find in Appendix A that the correlation coefficient between  $\mathbf{a}_j$  and  $\mathbf{b}_{j_w}$  is given by  $2p_w - 1$ . This indicates that the MU can control the strength of a *correlative* attack by adjusting its reflection probability  $p_w$ .

When  $p_w = \frac{1}{2}$ ,  $P_{A,B}(1,1) = P_A(1)P_B(1)$ , then  $\mathbf{a}_j$  and  $\mathbf{b}_{j_w}$  are independent, EVD-based methods can be used to estimate channels.

It is shown that the MUs do not need to explicitly know  $\mathbf{a}_j$ . By setting  $p_w \neq \frac{1}{2}$  when IRSs are used for random reflection, a *correlative* attack can be conducted. We proceed to analyze its effect below.

#### B. Detriment of Correlative Attack

In the pilot phase, after receiving  $\mathbf{Y}_p$ , the BS may estimate channels of the LUs by projecting  $\mathbf{Y}_p$  onto  $\mathbf{X}$ ,

$$\begin{aligned} [\tilde{\mathbf{h}}_1, \dots, \tilde{\mathbf{h}}_N] &= \mathbf{Y}_p \mathbf{X}^H \\ &= [\mathbf{h}_1, \dots, \mathbf{h}_N] + [\mathbf{g}_{1_1}, \dots, \mathbf{g}_{1_w}, \dots, \mathbf{g}_{N_1}, \dots, \mathbf{g}_{N_w}] \\ &\quad + \mathbf{N}_p \mathbf{X}^H, \end{aligned} \quad (6)$$

where the second equality relies on the orthogonal property of  $\mathbf{X}$ . This indicates that the pilot spoof attack causes the channel estimation to combine the legitimate and malicious channels. There is a large estimation error. It is difficult to obtain trustworthy CSI only using  $\mathbf{Y}_p$ . We propose to use  $\mathbf{Y}$  received during the data phase for channel estimation.

By collecting all the  $\mathbf{y}(t)$ ,  $1 \leq t \leq n$  in a transmission block, the received signal in the data phase can be recast as

$$\mathbf{Y} = \mathbf{C}\mathbf{S} + \mathbf{N}, \quad (7)$$

where  $\mathbf{Y} = [\mathbf{y}(1), \mathbf{y}(2), \dots, \mathbf{y}(n)]$ ,  $\mathbf{C} = [\mathbf{H}, \mathbf{G}]$ ,  $\mathbf{S} = \begin{bmatrix} \mathbf{A} \\ \mathbf{B} \end{bmatrix}$ ,  $\mathbf{H} = [\mathbf{h}_1, \mathbf{h}_2, \dots, \mathbf{h}_N]$ ,  $\mathbf{G} = [\mathbf{g}_{1_1}, \dots, \mathbf{g}_{1_w}, \dots, \mathbf{g}_{N_1}, \dots, \mathbf{g}_{N_w}]$ ,  $\mathbf{A} = \sqrt{P} [\mathbf{a}_1^T, \mathbf{a}_2^T, \dots, \mathbf{a}_N^T]^T$ ,  $\mathbf{B} = \sqrt{P} [\mathbf{b}_{1_1}^T, \dots, \mathbf{b}_{1_w}^T, \dots, \mathbf{b}_{N_1}^T, \dots, \mathbf{b}_{N_w}^T]^T$ .  $\mathbf{Y} \in \mathbb{C}^{M \times n}$ ,  $\mathbf{N} \in \mathbb{C}^{M \times n}$  are Gaussian noise, and each element follows  $\mathcal{CN}(0, \sigma^2)$ .

Traditional methods apply EVD to  $\frac{1}{Mn} \mathbf{Y} \mathbf{Y}^H$ . The resulting eigenspace is then used for jamming rejection when the jamming and legitimate data sequences are independent, i.e.,  $\frac{\mathbf{S} \mathbf{S}^H}{n} \xrightarrow{a.s.} \mathbf{I}_{N+WN}$ . However, under *correlative* attacks, due to (5), we have  $\frac{\mathbf{S} \mathbf{S}^H}{n} \xrightarrow{a.s.} \mathbf{R}_s \in \mathbb{C}^{(N+WN) \times (N+WN)}$ , where  $\mathbf{R}_s \neq \mathbf{I}_{N+WN}$ . We find that a *correlative* attack undermines the performance of an EVD-based method using the received signal  $\mathbf{Y}$  [8] [9].

**Proposition 1.** In a large-scale antenna regime, the right singular matrix of  $\frac{1}{Mn} \mathbf{Y} \mathbf{Y}^H$  is  $\mathbf{U}_Y = \frac{1}{\sqrt{M}} [\mathbf{U}_W, \mathbf{C} \mathbf{R}^{-\frac{1}{2}} \mathbf{U}_s]$ , where  $\mathbf{U}_W \in \mathbb{C}^{M \times (M-N-WN)}$  has orthogonal columns and spans the null space of  $[\mathbf{C} \mathbf{R}^{-\frac{1}{2}} \mathbf{U}_s]$ ,  $\mathbf{R} \in \mathbb{C}^{(N+WN) \times (N+WN)}$  is a diagonal matrix depending on  $\mathbf{C}$ ,  $\mathbf{U}_s \in \mathbb{C}^{(N+WN) \times (N+WN)}$  is an orthogonal matrix,  $\Lambda \in \mathbb{C}^{(N+WN) \times (N+WN)}$  is a diagonal matrix, and they are results of eigenvalue decomposition, i.e.,  $\mathbf{R}^{\frac{1}{2}} \mathbf{R}_s \mathbf{R}^{\frac{1}{2}} = \mathbf{U}_s \Lambda \mathbf{U}_s^H$ .

*Proof.* Please refer to Appendix B.  $\square$

**Remark 3:** Notice that  $\mathbf{U}_Y$  is determined by not only  $\mathbf{C} \mathbf{R}^{-\frac{1}{2}}$  but by  $\mathbf{U}_s$ .  $\mathbf{U}_s$  hinges on the degree of correlation among rows of  $\mathbf{S}$ . In [8] [9], all data streams are independent, i.e.,  $\mathbf{U}_s = \mathbf{I}$ . Then  $\mathbf{U}_Y$  is irrelevant to interference data.  $\mathbf{U}_Y$  is thus used to directly eliminate interference from MUs. However, in this paper, due to *correlative* attacks,  $\mathbf{U}_s \neq \mathbf{I}$ . The null space of MUs cannot be found from  $\mathbf{U}_Y$ , but the subspaces corresponding to MUs and LUs are united by  $\mathbf{U}_Y$ . This indicates that the MUs can directly manipulate  $\mathbf{U}_Y$  by conducting a *correlative* attack, hence past work no longer applies [8] [9].

As shown in (7), the received signals  $\mathbf{Y}$  are mixtures of  $\mathbf{S}$ , where the mixing matrix  $\mathbf{C}$  includes all channel vectors. Every element of noise distortion  $\mathbf{N}$  follows  $\mathcal{CN}(0, \sigma^2)$ ,  $\mathbf{N} \in \mathbb{C}^{M \times n}$ . This observation motivates us to restrict our goal of channel estimation to the field of blind signal separation (BSS). Nevertheless, due to the attack, there is a correlation between  $\mathbf{a}_j$  and  $\mathbf{b}_k$ , and the BS does not know the statistical characteristics of  $\mathbf{a}_j$  and  $\mathbf{b}_k$ . Traditional BSS techniques [16], [17] do not apply to the attack scenario considered in this paper. We next propose a BSS technique that works well under *correlative* attacks.

### IV. SIGNAL EXTRACTION AND CHANNEL ESTIMATION

For a *correlative* attack, we consider a geometric argument that is insensitive to correlation. For instance, the convex hull of  $\mathbf{uCS}$  [16], where  $\mathbf{u}$  is the normalized vector combination vector of  $\mathbf{CS}$ , only depends on the alphabet of  $\mathbf{uCS}$ , regardless of the correlation of  $\mathbf{S}$ . For ease of understanding, we illustrate convex hulls of sequences in Fig. 2.  $\mathcal{L}(\mathbf{uCS})$  achieves its minimum when  $\mathbf{uCS}$  includes only one data stream rather than the mixture of several streams, where  $\mathcal{L}(\cdot)$  denotes

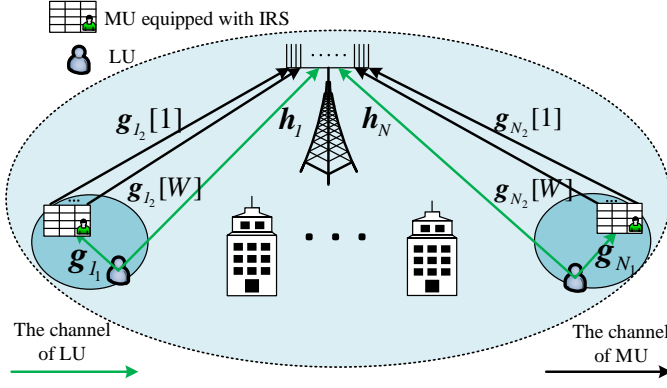


Fig. 1. System model including one BS equipped with  $M$  antennas and  $N$  group users. Each group includes one LU and one MU. Each MU is equipped with an IRS that includes  $W$  elements. Through the pilot and data phases, the MUs reflect  $W$  stream pilot sequences and interference sequences to the BS.

the length of the convex hull of its input sequence, i.e., the convex perimeter [16]. Hence, the convex perimeter can be used for signal extraction, which is also the basis of channel estimation. However, the BS receives only the noisy observation of  $\mathbf{CS}$ , i.e.,  $\mathbf{Y}$ , rather than  $\mathbf{CS}$  itself. The convex perimeter is very sensitive to noise. As seen in Fig. 2, the noise significantly changes the convex hull; hence, it impacts the convex perimeter. Proposition 2 provides an extractor capable of distilling alphabets from noisy observations.

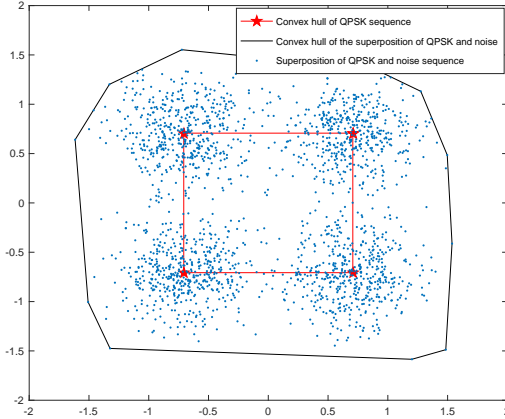


Fig. 2. Illustration of the constellation of QPSK sequences (dots) and QPSK and noise sequences (dots). Superimposed are the boundary and vertex of its convex hull; the noise changes the convex hull significantly.

**Proposition 2.** *Let us denote the alphabet of a discrete and  $n$ -length i.i.d. sequence  $V^n$  as  $\mathcal{V}$ . Another noise sequence  $W^n$  is independent of  $V^n$ . Then, from  $V^n + W^n$ , there exists an extractor  $\mathbb{F}$ , by whose use, i.e.,  $\mathbb{F}(V^n + W^n)$ ,  $\mathcal{V}$  can be extracted in probability as  $n$  approaches infinity.*

*Proof.* Proposition 2 is proved by the proposal of extractor  $\mathbb{F}$  in Appendix C.  $\square$

We use the extractor  $\mathbb{F}$  to distill  $\mathcal{V}$  from  $V^n + W^n$ . Since  $V^n$  is a discrete sequence, the convex perimeter of  $\mathcal{V}$  is equivalent

to that of  $V^n$ . We thus have Corollary 1, which is based on Proposition 2.

**Corollary 1.** *For a discrete and  $n$ -length i.i.d. sequence  $V^n$ , there is another noise sequence  $W^n$ , which is independent of  $V^n$ .  $\mathcal{L}\{\mathbb{F}\{V^n + W^n\}\} \rightarrow \mathcal{L}\{V^n\}$  in probability as  $n$  approaches infinity.*

We next use  $\mathbb{F}$  and  $\mathcal{L}$  to extract signals and estimate channels.

#### A. Signal Extraction

Revisiting (7),  $\mathbf{Y}$  is the superposition of  $\mathbf{CS}$  and the noise  $\mathbf{N}$ . Notice that signal extraction corresponds to the minimization of the convex perimeter of  $\mathbf{uCS}$  [16]. Relying on our proposed extractor  $\mathbb{F}$  to achieve the convex perimeter, we establish an optimization problem subject to the signal extraction vector, where  $\mathbf{u} \in \mathbb{C}^{1 \times M}$ ,

$$\begin{aligned} [\hat{\mathbf{u}}] &= \arg \{ \min \mathcal{L} \{ \mathbb{F} \{ \mathbf{uY} \} \} \} \\ \text{s.t. } &\|\mathbf{u}\|_2 = 1. \end{aligned} \quad (8)$$

Since

$$\mathbf{uY} = \mathbf{uCS} + \mathbf{uN},$$

according to Corollary 1,  $\mathcal{L}\{\mathbb{F}\{\mathbf{uY}\}\} \rightarrow \mathcal{L}\{\mathbf{uCS}\}$  in probability as  $n$  approaches infinity. The signal extraction vector is achieved by minimizing  $\mathcal{L}\{\mathbb{F}\{\mathbf{uY}\}\}$  [16]. As the contrast function of (8) reduces the impact of noise, problem (8) can be solved by traditional gradient descent [16]. Details can be found in Algorithm 1.

The key difference of our work is the employment of  $\mathbb{F}$  to reduce the impact of noise on the calculation of the convex perimeter. Previous work investigated the noiseless scenario, obtaining a signal extraction vector by minimizing the convex perimeter of  $\mathbf{uY}$  [16]. In our model, due to the existence of noise, we propose  $\mathbb{F}$  to obtain the convex perimeter of  $\mathbf{uCS}$ . Simulations confirm that  $\mathbb{F}$  significantly enhances extraction performance in the presence of a correlation attack and noise.

Based on (8), the signal of one user (LU or MU) is extracted as

$$\mathbf{s} = \hat{\mathbf{u}}\mathbf{Y}, \quad (9)$$

where  $\mathbf{s} \in \mathbb{C}^{1 \times n}$ . We next estimate one channel corresponding to the extracted  $\mathbf{s}$ .

#### B. Channel Estimation

Without loss of generality, we let  $\mathbf{c} \in \mathbb{C}^{M \times 1}$  denote the channel corresponding to the extracted  $\mathbf{s}$ . For  $m = 1 \dots M$ , we let  $[\cdot]_m$  denote the  $m$ th row of its input matrix or vector, and rewrite  $\mathbf{Y}$  as

$$[\mathbf{Y}]_m = [\mathbf{R}]_m + [\mathbf{c}]_m \mathbf{s}, \quad (10)$$

where  $\mathbf{R}$  is the remainder signal.

Both  $[\mathbf{R}]_m$  and  $[\mathbf{c}]_m \mathbf{s}$  are noisy observations that include noise and discrete sequences. Thus,  $[\mathbf{Y}]_m$  is the noisy mixture of sequences corresponding to  $[\mathbf{R}]_m$  and  $[\mathbf{c}]_m \mathbf{s}$ .  $\mathcal{L}$  achieves its local minimum value when its input is the alphabet of a single

signal rather than any mixture. Therefore, relying on  $\mathbb{F}$ ,  $\mathbf{c}$  can be estimated by

$$[\hat{\mathbf{c}}]_m = \arg \{ \min \mathcal{L} \{ \mathbb{F}([\mathbf{Y}]_m - \mathbf{c}'s) \} \}, \mathbf{c}' \in \mathbb{C}. \quad (11)$$

To solve this problem, we also prove that the solution is in a finite and discrete set, which leads to an optimum solution when searching the finite and discrete set.

**Proposition 3.** *The optimum solution to (11) is included in a finite and discrete set,  $\mathcal{Q}_m = \left\{ q \mid q = \frac{y-y'}{z-z'}, z \neq z', y \neq y', y, y' \in \mathcal{Y}_m, z, z' \in \mathcal{Z} \right\}$ , where  $\mathcal{Y}_m = \mathbb{F}([\mathbf{Y}]_m), \mathcal{Z} = \mathbb{F}\{s\}$ .*

*Proof.* Please refer to Appendix D.  $\square$

The key feature of (11) is the use of our proposed extractor  $\mathbb{F}$  in the contrast function of (11), and in Proposition 3 to locate a solution. Previous work [18] only considers a noiseless scenario and implements no denoising measures.

Based on Proposition 3, we can estimate  $\mathbf{c}$  as  $\hat{\mathbf{c}}$  from (11). Then, with  $\hat{\mathbf{c}}$  and the extracted  $\mathbf{c}$ , the contribution of  $s$  can be removed from  $\mathbf{Y}$ . After the deduction of  $\hat{\mathbf{c}}s$  from  $\mathbf{Y}$ , let us repeat the signal extraction and channel estimation, as presented in Algorithm 1, until all channels are estimated.

In Algorithm 1, steps 3~12 solve the optimization problem (8) by gradient descent. The resulting vector  $\hat{\mathbf{u}}$  is used for signal extraction in step 13. In steps 14~19, optimization problem (11) is solved by searching the discrete solution set given by Proposition 3. After  $s$  and  $\hat{\mathbf{c}}$  are obtained, we deduct  $\hat{\mathbf{c}}s$  from  $\mathbf{Y}$ , and iteratively run signal extraction and channel estimation.

### C. Channel Identification

Note that the proposed signal extraction depends on the minimum of  $\mathcal{L} \{ \mathbb{F}\{\mathbf{uY}\} \}$ , where  $\mathcal{L} \{ \mathbb{F}\{\mathbf{uY}\} \}$  remains unchanged when the angles of its input are rotated. Optimization problem (8) just indicates that the extracted signal belongs to one user, but it cannot determine which user corresponds to the extracted signal. Hence, order ambiguity exists.

Such ambiguities widely exist in BSS-based work [16] [19]. Previous work [19] assumes that the phase and order ambiguities are resolved perfectly by outdated estimate results. We similarly assume perfect channel identification.

## V. EXPERIMENTAL RESULTS

As the system model shows, there are  $N$  group users, each group includes one LU and one MU, and each MU is equipped with an IRS with  $W$  elements that can randomly reflect  $W$  stream signal sequences. The channel is i.i.d. Rayleigh fading, with an  $M \times (N + WN)$  channel matrix. Without loss of generality, we consider a massive MIMO system with  $M = 128$  antennas, and attack scenarios of  $N = 2, W = 2; N = 1, W = 3$ ; and  $N = 1, W = 1$ , as shown in Figs. 3, 4, and 5, respectively. The independent symbols of LUs are drawn from a BPSK constellation, and we assume that the MUs conduct the attack according to (3). When  $W = 1$ , we set  $\Pr\{\phi_{j_1} = 0\} = 0.8$ , and then the correlation coefficient of  $\mathbf{a}_j$  and  $\mathbf{b}_{j_1}$  is 0.6. When  $W = 2$ , we set  $\Pr\{\phi_{j_1} = 0\} = 0.6$ ,  $\Pr\{\phi_{j_2} = 0\} = 0.7$ . Then the correlation coefficients of  $\mathbf{a}_j$

### Algorithm 1: Signal Extraction and Channel Estimation

---

```

%  $i$ : the  $i$ th signal extraction and channel estimation;
%  $\mathbb{F}$ : our proposed extractor given by Algorithm 2 in
    Appendix C;
% convhull: the function of getting the convex points of
    its input sequence;
%  $\mathbb{P}$ : the function that finds  $\mathbf{uY}(p_1), \mathbf{uY}(p_2), \mathbf{uY}(\dots)$ ,
    and  $\mathbf{uY}(p_{n'})$  nearest to  $\mathbf{y}(k_1), \mathbf{y}(k_2), \mathbf{y}(\dots)$ , and  $\mathbf{y}(k_{n'})$ ,
    respectively;
Input:  $\mathbf{Y}, N, W, M$ 
Output: signals  $s_i$  and channels  $\hat{\mathbf{c}}_i$ , for
     $i = 1, 2, \dots, N_L + N_M$ 
1 for  $i = 1 : 1 : N + WN$  do
2   Initialization:  $\mathbf{u}(1) = 1, \mathbf{u}(2 : M) = 0$ ;
3   for  $iter = 1 : 1 : \text{until } \mathcal{L} \{ \mathbb{F}\{\mathbf{uY}\} \}$  minimum do
4      $\mathbf{y} = \mathbb{F}(\mathbf{uY})$  %  $\mathbf{y}$  is the alphabet of  $\mathbf{uY}$ 
5      $[k_1, k_2, \dots, k_{n'}] = \text{convhull}(\Re\{\mathbf{y}\}, \Im\{\mathbf{y}\})$ 
6      $\mathcal{L}(\mathbf{y}) = \sum_{i=2}^{n'} \|\mathbf{y}(k_i) - \mathbf{y}(k_{i-1})\|_2$ 
7      $[p_1, p_2, \dots, p_{n'}] = \mathbb{P} \{ [k_1, k_2, \dots, k_{n'}] \}$ 
8      $\mathbf{Wp} = \sum_{i=2}^{n'} \{ \mathbf{Y}(:, p_i) - \mathbf{Y}(:, p_{i-1}) \}$ 
9      $\{ \mathbf{Y}(:, p_i) - \mathbf{Y}(:, p_{i-1}) \}^H / (\|\mathbf{y}(k_i) - \mathbf{y}(k_{i-1})\|_2)$ 
10     $\mathbf{g} = (\frac{1}{2} \mathbf{Wp} \mathbf{u} - \mathbf{u} \mathcal{L}(\mathbf{y})) / \|\mathbf{u}\|_2$ 
11     $\mu = 1 / (2 \|\mathbf{g}\|_2^2)$ 
12     $\mathbf{u} = (\mathbf{u} - \mu \mathbf{g}) / \|\mathbf{u} - \mu \mathbf{g}\|_2$ 
13  end
14   $s_i = \hat{\mathbf{u}} \mathbf{Y}$  (9)
15   $\mathcal{Z}_i = \mathbb{F}(s_i)$ 
16  for  $m = 1 : 1 : M$  do
17     $\mathcal{Y}_m = \mathbb{F}([\mathbf{Y}]_m)$ 
18     $\mathcal{Q}_m = \left\{ q \mid q = \frac{y-y'}{z-z'}, z \neq z', y \neq y', y, y' \in \right.$ 
19     $\left. \mathcal{Y}_m, z, z' \in \mathcal{Z}_i \right\}$ 
20     $[\hat{\mathbf{c}}_i]_m = \arg \{ \min \mathcal{L} \{ \mathbb{F}([\mathbf{Y}]_m - \mathbf{c}'s_i) \} \}, \mathbf{c}' \in \mathcal{Q}_m$ 
21    (8)
22  end
    
```

---

and  $\mathbf{b}_{j_1}$  and of  $\mathbf{a}_j$  and  $\mathbf{b}_{j_2}$  are 0.2 and 0.4, respectively. When  $W = 3$ , we set  $\Pr\{\phi_{j_1} = 0\} = 0.6$ ,  $\Pr\{\phi_{j_2} = 0\} = 0.7$ ,  $\Pr\{\phi_{j_3} = 0\} = 0.8$ . Then the correlation coefficients of  $\mathbf{a}_j$  and  $\mathbf{b}_{j_1}$ ,  $\mathbf{a}_j$  and  $\mathbf{b}_{j_2}$ , and  $\mathbf{a}_j$  and  $\mathbf{b}_{j_3}$  are 0.2, 0.4, and 0.6, respectively. The BS estimates channels and achieves CSI. According to the achieved CSI, BS uses zero forcing (ZF) detection to get the signal-to-interference-and-noise ratio (SINR) of all users. The normalized mean square error (NMSE) of the channel estimation and the bit error rate (BER) of the separation signal are also selected as performance metrics. We simulate and compare the performance of our proposed method and those based on bounded component analysis (BCA) [16] and eigenvalue decomposition (EVD) [8]. We also simulate the performance achieved under perfect CSI. Since we consider multiple users, to evaluate the performance of every user, we use the mean-SINR, min-SINR, max-NMSE, mean-NMSE, and min-NMSE, where “mean,” “min,” and “max” respectively represent the average, worst, and best performance metrics

over all users.

Because the EVD-based method depends on the transmission power gap between LUs and MUs to get the separability of eigenspaces, we set the path-losses of MUs less than LUs, that means the interference of MUs in our proposed method is much stronger than that of EVD-based method. We use EVD-0.3 and EVD-0.5 denote the path-losses of MUs are 0.3 and 0.5, respectively.

In Figs. 3, 4, and 5, the path loss of MUs in the proposed method is 1. Although the interference of MUs in our proposed method was greater than the EVD-based method, the proposed method performs better than the EVD-based method, and our method performs close to the perfect CSI. Specifically, it is observed in Figs. 3, 4, and 5 that as the correlation coefficient is fixed, the performance of the EVD-based method remains almost unchanged despite an increase in the signal-to-noise ratio (SNR). In contrast, in Fig. 6, we consider  $N = 1, W = 1$ , and the performance of the EVD-based method changes significantly when the correlation coefficient of  $\mathbf{a}_j$  and  $\mathbf{b}_{j_1}$  increases from 0 to 0.8. Fig. 6 presents the performance of  $N = 1$  and  $W = 1$  under varying correlation coefficients with an SNR of 16 dB. The proposed method has better performance than the EVD-based method with different correlation coefficients. This is consistent with Proposition 1, indicating that in the presence of a *correlative* attack, the signals of LUs and MUs no longer lie in distinct eigenspaces of the received signal matrix in the BS. Instead, the subspace of the attack signals overlaps with the eigenspace corresponding to the LUs, thus leading to attack leakage when the EVD-based method employs eigenvectors corresponding to the LUs for the received signal projection.

In our proposed method, we consider reducing the impact of noise and use geometric properties to overcome the impact of a *correlative* attack. The performance increases as the SNR increases in Figs. 3, 4, and 5, and is unchanged in a certain range as the correlation coefficient increases in Fig. 6. Specifically, in Fig. 6(a), it is observed that when the correlation coefficient is 0.6, the SINR of the proposed method is better than that of the EVD-based method by more than 5 dB. The EVD-based method has better performance when the pass losses of MUs are less than that. This indicates that the stronger the attack signals, the worse the performance is of the EVD-based method. This could be because the EVD-based method attempts to eliminate attack signals as interference. The proposed method treats attack signals as those of regular users, rather than interference. We also estimate attack signals and channels instead of eliminating them as interference. Thus the proposed method outperforms the EVD-based method under much stronger attacks.

Next, in Figs. 3, 4, and 5, we present the performance of the BCA method, and we see that the proposed method performs much better. For instance, it is observed in Fig. 3 that the mean-SINR and min-SINR of the proposed method are better than those of the BCA method by more than 5 dB. The NMSE of the proposed method is better than that of the BCA method, especially at low SNRs.

To study the influence of signal correlation on performance, in Fig. 6(a), it is observed that the mean-SINR and min-

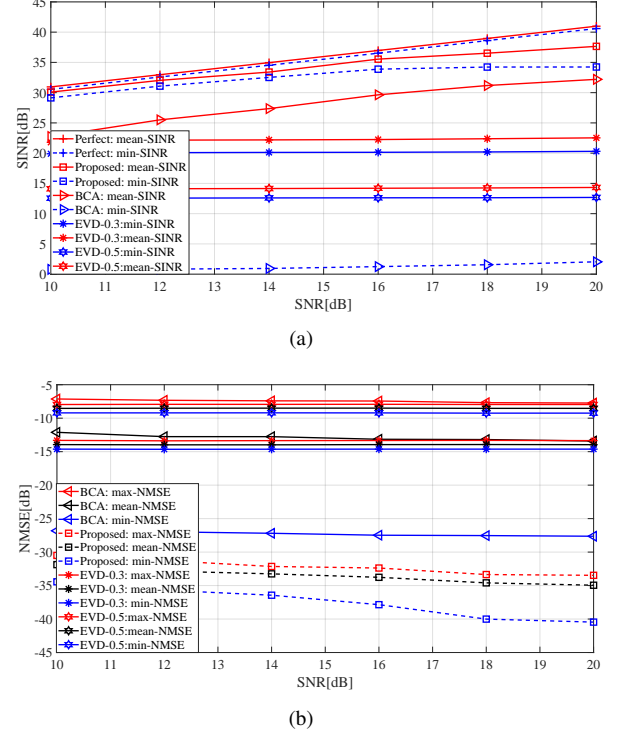


Fig. 3. (a) SINR and (b) NMSE of proposed, BCA, and EVD-based methods versus SNR with  $N = 2, W = 2$ . The correlation between signal sequences of LU and MU are fixed at 0.2 and 0.4, respectively.

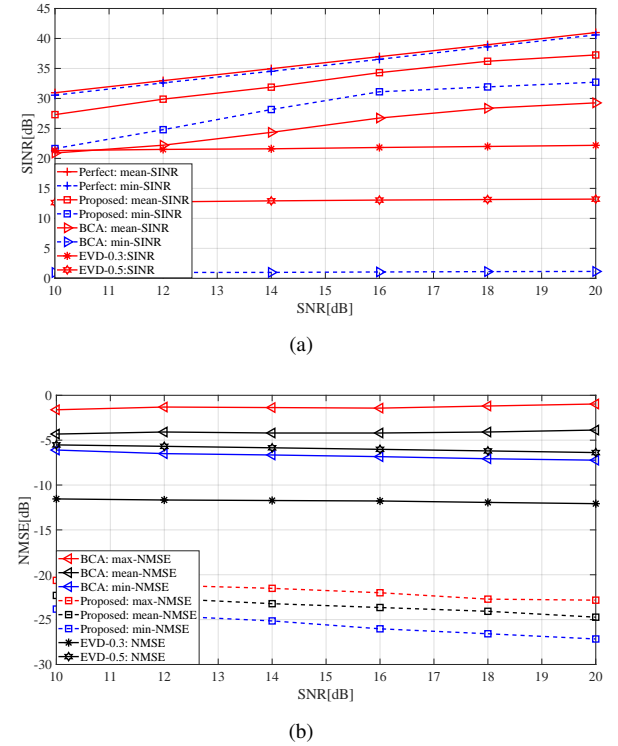


Fig. 4. (a) SINR and (b) NMSE of proposed, BCA, and EVD-based methods versus SNR with  $N = 1, W = 3$ . The correlation between signal sequences of LU and MU are fixed at 0.6, 0.7 and 0.8.



SINR of our proposed method outperform the BCA method by more than 5 dB, and the NMSE of the proposed method outperforms that of the BCA method. Fig. 7(a) shows the BER performance of  $N = 2, W = 2$ ;  $N = 1, W = 3$ ;  $N = 1, W = 1$  for the proposed method and BCA method. Fig. 7(b) shows the performance of  $N = 1, W = 1$  with different correlation coefficients. The proposed method outperforms the BCA method in any case.

We further discover that the performance of both methods, especially the BCA method, will deteriorate as the correlation coefficient increases. Actually, the BCA method works well in a noiseless scenario. This indicates that the BCA method is sensitive to noise, because it is based on geometric properties of desired signals. The existence of noise changes the shape of the convex hull of desired signals. Consequently, geometric properties cannot be captured exactly in the presence of noise. Therefore, the existence of Gaussian noise damages the performance of the BCA method against a dependence attack. In contrast, the performance of our proposed method changes little as the correlation of users' symbols increases. Our method considers the reduction of the impact of noise, as mentioned above, thus correlation does not significantly degrade its performance.

In summary, based on our simulation results, the proposed method outperforms the BCA and EVD-based methods in the sense of SINR, NMSE, and BER.

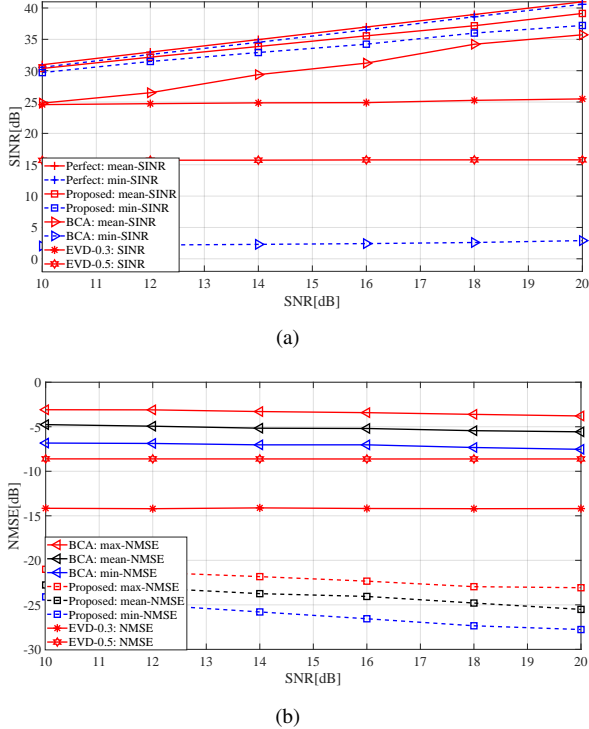


Fig. 5. (a) SINR and (b) NMSE of proposed, BCA, and EVD-based methods versus SNR with  $N = 1, W = 1$ . The correlation between LU and MU is fixed at 0.6.

## VI. CONCLUSION

Above all, we focus on channel estimation under a *correlative* attack with noise. We propose an extractor  $\mathbb{F}$  that can

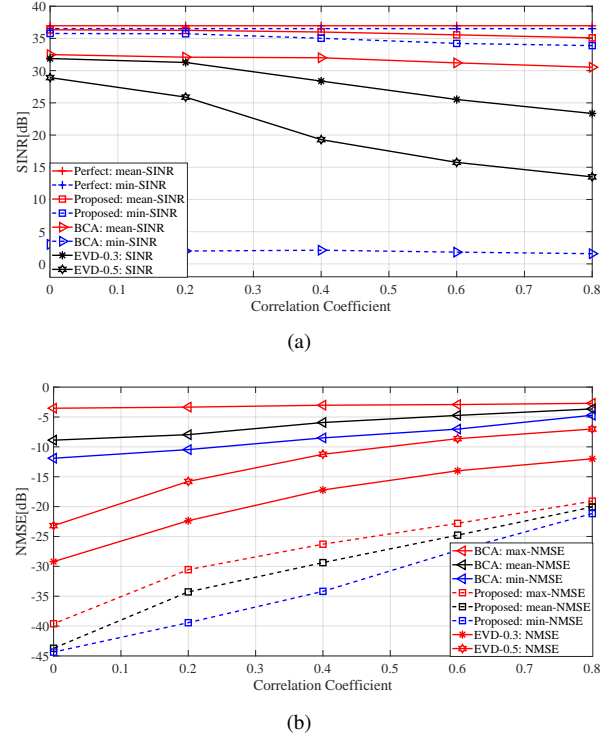


Fig. 6. (a) SINR and (b) NMSE of proposed, BCA, and EVD-based methods versus correlation coefficient with  $N = 1, W = 1$ . The SNR is fixed at 16 dB.

distill alphabets from a noisy signal. We apply this extractor to signal extraction and channel estimation. Numerical results show that the proposed method performs better than the BCA and EVD-based methods under a *correlative* attack in a noisy environment.

## APPENDIX A PROOF OF CORRELATION COEFFICIENT

When BPSK modulation is used by the signal sequence  $\mathbf{a} \in \mathbb{C}^{1 \times n}$ , it is not hard to obtain that  $P_A(1) = P_A(-1) = \frac{1}{2}$ .  $P_A$  denotes the stochastic distribution of  $\mathbf{a}$ . Due to the IRS,  $1 \leq t \leq n$ , and

$$\mathbf{b}(t) = \mathbf{a}(t)e^{i\phi}, \quad (12)$$

where  $\phi$  denotes the reflection phase of the IRS. It is randomly set according to  $\Pr\{\phi = 0\} = p$ ,  $\Pr\{\phi = \pi\} = 1 - p$ .  $\mathbf{a}(t), \mathbf{b}(t)$  are the respective  $t$ th elements in  $\mathbf{a}, \mathbf{b}$ . Then the transition probability  $P_{B|A}(1|1) = P_{B|A}(-1|-1) = p$ ,  $P_{B|A}(-1|1) = P_{B|A}(1|-1) = 1 - p$ . Then in  $\mathbf{b}$ ,

$$\begin{aligned} P_B(1) &= P_A(1)P_{B|A}(1|1) + P_A(-1)P_{B|A}(1|-1) \\ &= \frac{1}{2}p + \frac{1}{2}(1 - p) = \frac{1}{2}. \end{aligned} \quad (13)$$

$$P_B(-1) = 1 - P_B(1) = \frac{1}{2}. \quad (14)$$

$P_B$  denotes the stochastic distribution of  $\mathbf{b}$ .  $\bar{\mathbf{a}}$  and  $\bar{\mathbf{b}}$  are 0 as  $n$  approaches infinity,  $\bar{(\cdot)}$  denotes the mean value of its input sequence. Then the correlation coefficient of  $\mathbf{a}$  and  $\mathbf{b}$  is

$$\rho_{ab} = \frac{\sum_{t=1}^n (\mathbf{a}(t) - \bar{\mathbf{a}})(\mathbf{b}(t) - \bar{\mathbf{b}})}{\sqrt{\sum_{t=1}^n (\mathbf{a}(t) - \bar{\mathbf{a}})^2} \sqrt{\sum_{t=1}^n (\mathbf{b}(t) - \bar{\mathbf{b}})^2}} \quad (15)$$

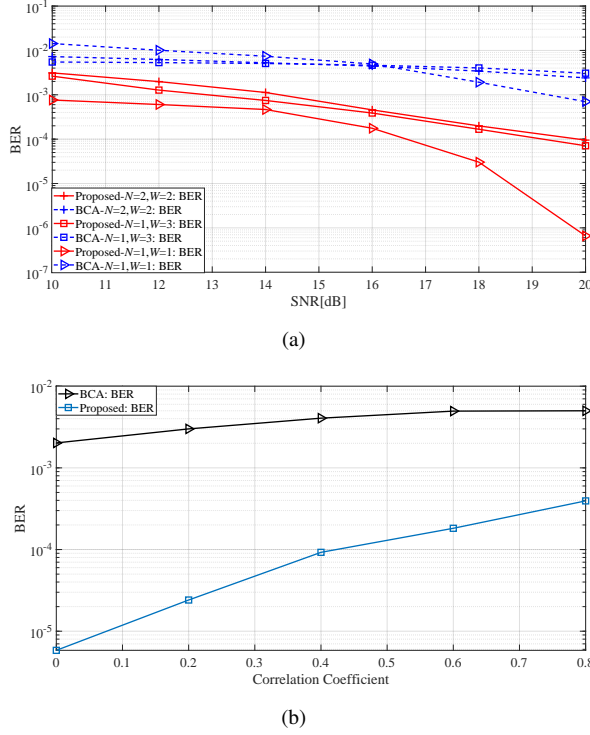


Fig. 7. BER of proposed method and BCA method: (a)  $N = 2, W = 2$ ;  $N = 1, W = 3$ ;  $N = 1, W = 1$ . (b)  $N = 1, W = 1$ . SNR is fixed at 16 dB.

$$\begin{aligned}
&= \frac{\sum_{t=1}^n \mathbf{a}(t)\mathbf{b}(t)}{\sqrt{\sum_{t=1}^n \mathbf{a}(t)^2} \sqrt{\sum_{t=1}^n \mathbf{b}(t)^2}} = \frac{pn - (1-p)n}{n} \\
&= 2p - 1.
\end{aligned}$$

## APPENDIX B PROOF OF PROPOSITION 1

According to [20], Corollary 1], we obtain  $\frac{1}{M}\mathbf{H}^H\mathbf{H} \xrightarrow{a.s.} \frac{1}{M}\text{Tr}(\mathbf{R}_H)$ ,  $\frac{1}{M}\mathbf{G}^H\mathbf{G} \xrightarrow{a.s.} \frac{1}{M}\text{Tr}(\mathbf{R}_G)$ ,  $\frac{1}{M}\mathbf{G}^H\mathbf{H} \xrightarrow{a.s.} 0$ ,  $\frac{1}{M}\mathbf{H}^H\mathbf{G} \xrightarrow{a.s.} 0$ . Then we have  $\frac{1}{M}\mathbf{C}^H\mathbf{C} \xrightarrow{a.s.} \frac{1}{M}\begin{bmatrix} \text{Tr}(\mathbf{R}_H) & 0 \\ 0 & \text{Tr}(\mathbf{R}_G) \end{bmatrix} = \mathbf{R}$ , and  $\mathbf{U}_Y^H\mathbf{U}_Y \xrightarrow{a.s.} \mathbf{I}_M$ . Because the distribution of  $\mathbf{S}$  is independent and identical, we have  $\frac{\mathbf{S}\mathbf{S}^H}{n} \xrightarrow{a.s.} \mathbf{R}_s$ . Then we decompose  $\mathbf{R}_Y$  as

$$\begin{aligned}
\mathbf{R}_Y &= \frac{1}{M}\mathbf{C}\mathbf{R}_s\mathbf{C}^H + \frac{\sigma^2}{M}\mathbf{I}_M \\
&= \frac{1}{M}\mathbf{C}\mathbf{R}^{-\frac{1}{2}}\mathbf{R}^{\frac{1}{2}}\mathbf{R}_s\mathbf{R}^{\frac{1}{2}}\mathbf{R}^{-\frac{1}{2}}\mathbf{C}^H + \frac{\sigma^2}{M}\mathbf{I}_M \\
&\stackrel{(a)}{=} \frac{1}{M}\mathbf{C}\mathbf{R}^{-\frac{1}{2}}\mathbf{U}_s\Lambda\mathbf{U}_s^H\mathbf{R}^{-\frac{1}{2}}\mathbf{C}^H + \frac{\sigma^2}{M}\mathbf{I}_M \\
&\xrightarrow{a.s.} \frac{1}{M}\mathbf{C}\mathbf{R}^{-\frac{1}{2}}\mathbf{U}_s\Lambda\mathbf{U}_s^H\mathbf{R}^{-\frac{1}{2}}\mathbf{C}^H + \frac{\sigma^2}{M}\mathbf{U}_Y\mathbf{U}_Y^H \\
&= \frac{1}{M}\mathbf{C}\mathbf{R}^{-\frac{1}{2}}\mathbf{U}_s\Lambda\mathbf{U}_s^H\mathbf{R}^{-\frac{1}{2}}\mathbf{C}^H + \frac{\sigma^2}{M}\mathbf{U}_W\mathbf{U}_W^H + \\
&\quad \frac{\sigma^2}{M}\mathbf{C}\mathbf{R}^{-\frac{1}{2}}\mathbf{U}_s\mathbf{U}_s^H\mathbf{R}^{-\frac{1}{2}}\mathbf{C}^H \\
&= \mathbf{U}_Y\text{diag}\{\sigma^2\mathbf{I}_{M-N-WN}, \Lambda + \sigma^2\mathbf{I}_{N+WN}\}\mathbf{U}_Y^H.
\end{aligned} \tag{16}$$

As long as  $n$  is sufficiently large,  $\mathbf{R}_Y$  can be approached by  $\frac{1}{Mn}\mathbf{Y}\mathbf{Y}^H$ . The convergence follows  $\mathbf{U}_Y\mathbf{U}_Y^H \xrightarrow{a.s.} \mathbf{I}_M$ , and the equation (a) follows  $\mathbf{R}^{\frac{1}{2}}\mathbf{R}_s\mathbf{R}^{\frac{1}{2}} = \mathbf{U}_s\Lambda\mathbf{U}_s^H$ .

## APPENDIX C PROOF OF PROPOSITION 2

Due to space limitations, we sketch the proof of Proposition 2 and present an algorithm to implement it. We use  $L^n$  to denote  $V^n + W^n$ . Note that  $L^n, V^n, W^n$  are i.i.d. random sequences. Let  $V$  denote a generic random variable with the same stochastic distribution as each element of  $V^n$ . Similarly, we use generic random variables  $W$  and  $L$  following stochastic distributions identical to those of elements of  $W^n$  and  $L^n$ , respectively. Furthermore, note that  $W^n$  and  $V^n$  are independent of each other. As a consequence,  $W$  is independent of  $V$ . Since  $L^n = V^n + W^n$ , we specify  $L$  by  $L = V + W$ . Let  $F_L, F_V$ , and  $F_W$  denote the distributions of  $L, V$ , and  $W$ , respectively. Then, because  $V$  and  $W$  are independent of each other, we have

$$\Phi_{F_L}(\mathbf{f}) = \Phi_{F_V}(\mathbf{f})\Phi_{F_W}(\mathbf{f}), \tag{17}$$

where  $\Phi_F(\mathbf{f})$  denotes the characteristic function (CF) of the distribution  $F$ , and  $\mathbf{f}$  is the frequency vector. Note that the noise variance parameter  $\sigma_W^2$  is a characteristic of the receiver circuitry and can be measured *a priori*. We may assume that its value is known; hence,  $\Phi_{F_W}(\mathbf{f}) = \exp\{-2\sigma_W^2\pi^2|\mathbf{f}|^2\}$  is also known. Therefore, according to (17),  $F_U$  is achieved by

$$F_V = \Phi^{-1}\left(\frac{\Phi_{F_L}(\mathbf{f})}{\exp\{-2\sigma_W^2\pi^2|\mathbf{f}|^2\}}\right), \tag{18}$$

where  $\Phi^{-1}(\cdot)$  denotes the inverse CF of its input. It is worth noting that in (18),  $F_V$  is perfectly obtained from  $L$ , even though  $L$  includes noise  $W$  with arbitrary average power  $\sigma_W^2$ .  $V$  has a discrete alphabet  $\mathcal{V}$  that can be achieved by finding points  $\mathbf{v}$  that make  $F_V(\mathbf{v}) > 0$ . As a result, the extractor given by (18) satisfies our goal of extracting alphabets from noisy observations. However, in practice, to implement (18) is a challenge for two reasons.

- 1) Due to attack,  $F_L$  is unknown. The lack of  $F_L$  leads the inability to obtain  $\Phi_{F_L}(\omega)$  exactly.
- 2)  $\Phi(\cdot)$  and  $\Phi^{-1}(\cdot)$  correspond to a continuous Fourier transform (CFT) and inverse CFT, respectively. The transforms over a continuous domain may give rise to issues of implementation.

Motivated by these two challenges, we propose an extractor according to (18) by using a quantized empirical distribution of  $L^n$  to approach  $F_L$  according to the law of large numbers (LLN), and using a discrete Fourier transform (DFT) and inverse DFT to approach  $\Phi(\cdot)$  and  $\Phi^{-1}(\cdot)$ , respectively. According to LLN and the Nyquist sampling theorem, the approximation of  $\Phi_{F_L}(\mathbf{f})$  becomes more accurate as the quantization level and number of observations increase. In this sense, on the basis of (18), Proposition 2 has been proved. Furthermore, we provide an algorithm to implement (18) by sequential quadratic programming (SQP). To be more precise, notice that (18) is equivalent to

$$F_V(v) = \arg \min_{\hat{F}_V} \iint \left| \Phi_{F_L}(\mathbf{f}) - \Phi_{\hat{F}_V}(\mathbf{f})\Phi_{F_W}(\mathbf{f}) \right|^2 d\mathbf{f}, \tag{19}$$



where  $\hat{F}_V$  is a stochastic distribution function. To approximate  $\Phi_{F_L}(\mathbf{f})$ , we quantize  $L$  and achieve an empirical distribution,

$$\Pi_{\hat{L}^n}(n_1, n_2) = \frac{1}{n} \sum_{i=1}^n \mathbf{1}\{\Re\{L_i\} \in \mathcal{B}(n_1)\} \mathbf{1}\{\Im\{L_i\} \in \mathcal{B}(n_2)\}, \quad (20)$$

where  $L_i$  is the  $i$ -th variable of  $L^n$ ;  $\Re\{\cdot\}$  and  $\Im\{\cdot\}$  denote the real and imaginary parts, respectively, of its input; and  $\mathbf{1}\{\cdot\}$  is an indicator function.  $\mathcal{B}(n_1) = [-d_1 + n_1\Delta, -d_1 + (n_1 + 1)\Delta]$ ,  $\Delta = \frac{2d_1}{n_1}$ ,  $d_1 = \sqrt{n_1}$ . For  $\mathbf{f} = [f_r, f_i]$ ,  $\Phi_{F_L}(\mathbf{f})$  could be approached by

$$\begin{aligned} \Phi_{F_L}(\mathbf{f}) &= \int F_L(l) \exp\left\{-i2\pi\mathbf{f} \begin{bmatrix} \Re(l) \\ \Im(l) \end{bmatrix}\right\} dl \\ &\stackrel{N, n \rightarrow \infty}{\rightarrow} \Delta^2 \exp\{i2\pi(f_r + f_i)d_1\} \\ &\times \sum_{n_1=1}^N \sum_{n_2=1}^N \Pi_{\hat{L}^n}(n_1, n_2) \exp\{-i2\pi n_1 \Delta f_r\} \exp\{-i2\pi n_2 \Delta f_i\}. \end{aligned} \quad (21)$$

Sampling  $\Phi_{F_L}(\mathbf{f})$  across  $(k_1 f, k_2 f)$ ,  $k_1, k_2 = 1, \dots, N_f$ ,  $f = \frac{1}{\Delta N_f}$ , we have

$$\begin{aligned} \Phi_{F_L}(k_1 f, k_2 f) &\stackrel{N, n \rightarrow \infty}{\rightarrow} \tilde{\Phi}_{F_L}(k_1 f, k_2 f) \\ &= \Delta^2 \exp\left\{i2\pi\left(\frac{k_1}{\Delta N_f} + \frac{k_2}{\Delta N_f}\right)d_1\right\} \\ &\times \underbrace{\sum_{n_1=1}^N \sum_{n_2=1}^N \Pi_{\hat{L}^n}(n_1, n_2) \exp\left\{-i2\pi\frac{n_1 k_1}{N_f}\right\} \exp\left\{-i2\pi\frac{n_2 k_1}{N_f}\right\}}_{[\text{DFT}\{\Pi_{\hat{L}^n}\}]_{k_1, k_2}}, \end{aligned}$$

where  $\tilde{\Phi}_{F_L}(k_1 f, k_2 f)$  can be obtained from the DFT of  $\Pi_{\hat{L}^n}$ , denoted by  $\text{DFT}\{\Pi_{\hat{L}^n}\}$ , which is an  $N_f \times N_f$  matrix whose  $(k_1, k_2)$ -th element corresponds to the value of  $\text{DFT}\{\Pi_{\hat{L}^n}\}$  in the  $(k_1, k_2)$ -th frequency. Hence, we approximate  $\Phi_{F_L}(\mathbf{f})$  by an  $N_f \times N_f$  matrix  $\mathbf{L}$  whose  $(k_1, k_2)$ -th element is

$$[\mathbf{L}]_{k_1, k_2} = \Delta^2 \exp\left\{i2\pi\left(\frac{k_1}{\Delta N_f} + \frac{k_2}{\Delta N_f}\right)d_1\right\} [\text{DFT}\{\Pi_{\hat{L}^n}\}]_{k_1, k_2}. \quad (22)$$

Similarly,  $\Phi_{F_V}(\mathbf{f})$  can be approximated by an  $N_f \times N_f$  matrix  $\mathbf{V}$  whose  $(k_1, k_2)$ -th element is

$$[\mathbf{V}]_{k_1, k_2} = \Delta^2 \exp\left\{i2\pi\left(\frac{k_1}{\Delta N_f} + \frac{k_2}{\Delta N_f}\right)d_1\right\} [\text{DFT}\{\Pi_{\hat{V}^n}\}]_{k_1, k_2}. \quad (23)$$

$\Pi_{\hat{V}^n}$  is the empirical distribution of the quantized sequence of  $V^n$ , similar to  $\Pi_{\hat{L}^n}$  (20). Furthermore, according to the definition of DFT, we extend  $\text{DFT}\{\Pi_{\hat{V}^n}\}$  by

$$\text{DFT}\{\Pi_{\hat{V}^n}\} = \mathbf{F} \Pi_{\hat{V}^n} \mathbf{F}^T, \quad (24)$$

where  $\mathbf{F} \in \mathbb{C}^{N_f \times N}$ ,  $[\mathbf{F}]_{i,j} = \exp(-j2\pi(i-1)(j-1)/N_f)$ ,  $i = 1, \dots, N$ ,  $j = 1, 2, \dots, N_f$ . Substituting (24) in (23), we have

$$\mathbf{V} = \mathbf{R}_V \odot \{\mathbf{F} \Pi_{\hat{V}^n} \mathbf{F}^T\}, \quad (25)$$

where  $\mathbf{R}_V \in \mathbb{C}^{N_f \times N_f}$ ,  $[\mathbf{R}_V]_{k_1, k_2} = \Delta^2 \exp\left\{i2\pi\left(\frac{k_1}{\Delta N_f} + \frac{k_2}{\Delta N_f}\right)d_1\right\}$ ,  $k_1, k_2 = 1, \dots, N_f$ , and  $\odot$  denotes the dot product. Notice that  $\Phi_{F_L}(\mathbf{f})$  and  $\Phi_{F_V}(\mathbf{f})$  can be approximated by  $\mathbf{L}$  and  $\mathbf{V}$ , respectively. Based on (17), we have

$$\mathbf{L} \approx \mathbf{R}_W \odot \mathbf{R}_V \odot \{\mathbf{F} \Pi_{\hat{V}^n} \mathbf{F}^T\}, \quad (26)$$

where  $\mathbf{R}_W \in \mathbb{C}^{N_f \times N_f}$  samples  $\Phi_{F_W}(\mathbf{f})$ ,  $[\mathbf{R}_W]_{k_1, k_2} = \exp\{-2\sigma_W^2 \pi^2 |k_1^2 + k_2^2| f^2\}$ . Then (17) further indicates that (19) can be transformed to a matrix form,

$$\tilde{F}_V = \arg \min_{\tilde{F}_V} \left| \mathbf{L} - \mathbf{R}_W \odot \mathbf{R}_V \odot \{\mathbf{F} \tilde{F}_V \mathbf{F}^T\} \right|^2, \quad (27)$$

where  $\tilde{F}_V \in \mathbb{C}^{N \times N}$  is a stochastic matrix to characterize the distribution over a complex domain. We use SQP to solve (27). The points making  $\tilde{F}_V$  achieve local maxima are extracted as the estimate of  $\mathcal{V}$ . As  $n$ ,  $N$ , and  $N_f$  increase, (27) approximates (19) more accurately. As a beneficial result, the extracted points from  $\tilde{F}_V$  converge to  $\mathcal{V}$  in probability. We define the proposed extractor as  $\mathbb{F}$ , whose steps are summarized by Algorithm 2, which can be run several times to achieve convergence.

---

**Algorithm 2:**  $\mathbb{F}$ : Extraction of Alphabets from a Noisy Sequence  $L^n$

---

- 1: Get  $\Pi_{\hat{L}^n}$  from  $L^n$  according to (20)
  - 2: Get  $\mathbf{L}$  according to (22)
  - 3: Set up optimization problem (27)  
 $\tilde{F}_V = \arg \min_{\tilde{F}_V} \left| \mathbf{L} - \mathbf{R}_W \odot \mathbf{R}_V \odot \{\mathbf{F} \tilde{F}_V \mathbf{F}^T\} \right|^2$
  - 4: Invoking SQP method to solve (27)
  - 5: Based on  $\tilde{F}_V$ , find the local maximum points for extracting alphabet.
- 

## APPENDIX D PROOF OF PROPOSITION 3

We notice that the optimized signal extraction vector  $\hat{\mathbf{u}}$  only extracts the signal of one user,  $\mathbf{s}$ . Further, estimate the corresponding channel  $\mathbf{c}$ . Then we rewrite  $\mathbf{Y}$  as

$$\mathbf{Y} = \mathbf{R} + \mathbf{c}\mathbf{s}, \quad (28)$$

where  $\mathbf{R}$  is the remainder signal. More precisely, we choose the  $m$ th row of  $\mathbf{Y}$ , where  $[\cdot]_m$  denotes the  $m$ th row of its input matrix or vector,

$$[\mathbf{Y}]_m = [\mathbf{R}]_m + [\mathbf{c}]_m \mathbf{s}. \quad (29)$$

Since the noise exists, we use the extractor  $\mathbb{F}$  to distill alphabets and obtain the alphabets of (29) as

$$\mathcal{Y}_m = \{y | y = \gamma + [\mathbf{c}]_m \mathbf{z}, \mathbf{z} \in \mathcal{Z}, \gamma \in \mathcal{R}\}, \quad (30)$$

where  $\mathcal{Y}_m = \mathbb{F}\{[\mathbf{Y}]_m\}$ ,  $\mathcal{Z} = \mathbb{F}\{\mathbf{s}\}$ , and  $\mathcal{R} = \mathbb{F}\{[\mathbf{R}]_m\}$ . We discover that all the different pairwise elements  $(y - y')$  chosen from  $\mathcal{Y}_m$  must contain the element  $[\mathbf{c}]_m(\mathbf{z} - \mathbf{z}')$ . Finally, we can obtain the finite set of  $[\mathbf{c}]_m$  as

$$\mathcal{Q}_m = \left\{ q \mid q = \frac{y - y'}{z - z'}, z \neq z', y \neq y', y, y' \in \mathcal{Y}_m, z, z' \in \mathcal{Z} \right\}. \quad (31)$$

## REFERENCES

- [1] M. Jordo and N. B. Carvalho, "Massive mimo antenna transmitting characterization," in *2018 IEEE MTT-S International Microwave Workshop Series on 5G Hardware and System Technologies (IMWS-5G)*, pp. 1–3, Aug 2018.
- [2] Q. Xiong, Y. Liang, K. H. Li, Y. Gong, and S. Han, "Secure transmission against pilot spoofing attack: A two-way training-based scheme," *IEEE Transactions on Information Forensics and Security*, vol. 11, pp. 1017–1026, May 2016.
- [3] Y. Wu, A. Khisti, C. Xiao, G. Caire, K. Wong, and X. Gao, "A survey of physical layer security techniques for 5g wireless networks and challenges ahead," *IEEE Journal on Selected Areas in Communications*, vol. 36, pp. 679–695, April 2018.
- [4] T. T. Do, E. Bjrnson, E. G. Larsson, and S. M. Razavizadeh, "Jamming-resistant receivers for the massive mimo uplink," *IEEE Transactions on Information Forensics and Security*, vol. 13, pp. 210–223, Jan 2018.
- [5] H. Wang, K. Huang, and T. A. Tsiftsis, "Multiple antennas secure transmission under pilot spoofing and jamming attack," *IEEE Journal on Selected Areas in Communications*, vol. 36, pp. 860–876, April 2018.
- [6] F. Bai, P. Ren, Q. Du, and L. Sun, "A hybrid channel estimation strategy against pilot spoofing attack in miso system," in *2016 IEEE 27th Annual International Symposium on Personal, Indoor, and Mobile Radio Communications (PIMRC)*, pp. 1–6, Sep. 2016.
- [7] J. Xie, Y. Liang, J. Fang, and X. Kang, "Two-stage uplink training for pilot spoofing attack detection and secure transmission," in *2017 IEEE International Conference on Communications (ICC)*, pp. 1–6, May 2017.
- [8] Y. Wu, C. Wen, W. Chen, S. Jin, R. Schober, and G. Caire, "Data-aided secure massive mimo transmission under the pilot contamination attack," *IEEE Transactions on Communications*, vol. 67, pp. 4765–4781, July 2019.
- [9] W. Wang, N. Cheng, K. C. Teh, X. Lin, W. Zhuang, and X. Shen, "On countermeasures of pilot spoofing attack in massive mimo systems: A double channel training based approach," *IEEE Transactions on Vehicular Technology*, vol. 68, pp. 6697–6708, July 2019.
- [10] D. Mishra and E. G. Larsson, "Passive intelligent surface assisted mimo powered sustainable iot," in *ICASSP 2020 - 2020 IEEE International Conference on Acoustics, Speech and Signal Processing (ICASSP)*, pp. 8961–8965, 2020.
- [11] M. Cui, G. Zhang, and R. Zhang, "Secure wireless communication via intelligent reflecting surface," *IEEE Wireless Communications Letters*, vol. 8, no. 5, pp. 1410–1414, 2019.
- [12] Z. Chu, W. Hao, P. Xiao, and J. Shi, "Intelligent reflecting surface aided multi-antenna secure transmission," *IEEE Wireless Communications Letters*, vol. 9, no. 1, pp. 108–112, 2020.
- [13] D. Darsena, G. Gelli, I. Iudice, and F. Verde, "Design and performance analysis of channel estimators under pilot spoofing attacks in multiple-antenna systems," *IEEE Transactions on Information Forensics and Security*, vol. 15, pp. 3255–3269, 2020.
- [14] Q. Wu and R. Zhang, "Towards smart and reconfigurable environment: Intelligent reflecting surface aided wireless network," *IEEE Communications Magazine*, vol. 58, pp. 106–112, January 2020.
- [15] Q. Wu and R. Zhang, "Beamforming optimization for wireless network aided by intelligent reflecting surface with discrete phase shifts," *IEEE Transactions on Communications*, vol. 68, no. 3, pp. 1838–1851, 2020.
- [16] S. Cruces, "Bounded component analysis of linear mixtures: A criterion of minimum convex perimeter," *IEEE Transactions on Signal Processing*, vol. 58, pp. 2141–2154, April 2010.
- [17] A. T. Erdogan, "A class of bounded component analysis algorithms for the separation of both independent and dependent sources," *IEEE Transactions on Signal Processing*, vol. 61, pp. 5730–5743, Nov 2013.
- [18] P. Aguilera, S. Cruces, I. Durn-Daz, A. Sarmiento, and D. P. Mandic, "Blind separation of dependent sources with a bounded component analysis deflationary algorithm," *IEEE Signal Processing Letters*, vol. 20, pp. 709–712, July 2013.
- [19] J. K. Tugnait, "Pilot spoofing attack detection and countermeasure," *IEEE Transactions on Communications*, vol. 66, pp. 2093–2106, May 2018.
- [20] J. Evans and D. N. C. Tse, "Large system performance of linear multiuser receivers in multipath fading channels," *IEEE Transactions on Information Theory*, vol. 46, no. 6, pp. 2059–2078, 2000.